Low-Cost and Aerodynamics-Aim Hypersonic Flight Experiment MF-1

Han-shan Xiao, Chao Ou [a], Hong-liang Ji, Zheng-chun He, Ning-yuan Liu and Xian-xu Yuan

China Aerodynamic Research and Development Center, China

Abstract. For increasing understanding of fundamental hypersonic phenomena, the flight test program, named MF-1, is to gather fundamental scientific and engineering data on the physics and technologies critical to future operational hypersonic flight with low-cost flight test platform, which is built on the retrofitted rockets. The MF-1 program is a hypersonic flight test program executed by China Aerodynamic Research and Development Center (CARDC). The MF-1 flight flew in December 2015. The flight focuses primarily on integration of instrumentation on the test vehicle, with application to boundary layer transition and shock interaction experiments. The MF-1 payload consists of a blunted 7° half angle cone, a cylinder and 33° flare configuration. The payload was boosted to Mach 5.32 utilizing a solid-rocket booster without control for the whole flight. The flight was fully successful, and measured transition under supersonic and hypersonic conditions. The heat flux data were given by the three-dimensional thermal identification method to discriminate transition zone. The preliminary analysis shows that the real-time flight data obtained by MF-1 are reliable and can be used to validate the transition predicting model and software. The results show that the existing model is able to predict the transition location of cone at a small angle-of-attack for supersonic or hypersonic flow. This paper describes the MF-1 mission and some general conclusions derived from the experiment.

1 Introduction

The MF-1 program is a hypersonic flight test program executed by China Aerodynamic Research and Development Center. MF-1 is the experimental flight with the primary experiment focused on boundary layer transition (BLT) on the low cost flight test vehicle. The corresponding secondary experiment is turbulent separated shock boundary layer interaction (SBLI). The research effort will consist of a series of focused tasks to resolve hypersonic phenomena through validation of computational analysis, comparison with performance predictions, enhancement of design data bases, and development of correlations with ground test[1].

Boundary layer transition has an important impact on hypersonic vehicle aerodynamics and aerothermodynamics. It is an inherently challenging problem due to its nonlinear nature and sensitivity to initial and boundary conditions. Ground test of boundary layer transition is generally unsatisfactory due to the high noise levels of ground facilities compared to flight. Computation is challenging since it requires resolution of instabilities of relatively high wavenumber and frequency over large spatial domains. Flight provides the best environment for measuring transition. Instrumentation for the flight environment however, is challenging. Careful measurement and computation of boundary conditions will provide added value in interpreting the data[2-3].

In recent years, a large number of flight tests have been carried out for hypersonic boundary transition and shock-border layer interference[4-5]. Such as the Hypersonic International Flight Research Experimentation (HIFiRE) program jointly implemented by the Air Force Research Laboratory (AFRL) of the United States and Australian Defence Science and Technology Group (DSTG), with a total of 3 flight tests dedicated to related issues (HIFiRE-1, 5, 9). As well as the Sharp Edge Flight Experiment program (SHEFEX) implemented by the German Aerospace Center (DLR), the SHEFEX-1 and 2 flight tests have been completed. Fig. 1 and Fig. 2 are typical research loads for HIFiRE and SHEFEX[6-13].

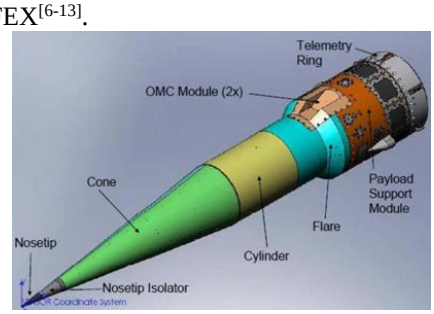

Figure 1. The payload of HIFiRE-1.

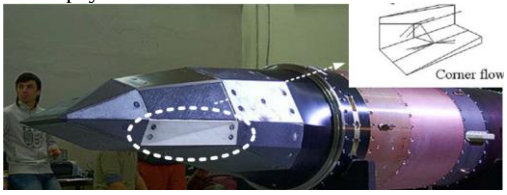

Figure 2. Shock-Border Layer Interference Load of SHEFEX.

[a] Corresponding author: hezhengchun@cardc.cn

The features which make the current experiment novel are the potential for hypersonic measurement, controlled roughness, or angle of attack measurements, and application of modern analysis. Improvements in modelling can now derive more consistent transition criteria from a flight experiment. In addition, historic experiments often did not record vehicle attitude or nose geometry, leading to increased uncertainty. Accurate knowledge of the vehicle attitude in the MF-1 flight is required to fully understand the BLT results.

MF-1 was launched on December 30 at 16:00:00 Beijing time in 2015. Telemetry data was received for the entire flight. This mission was entirely successful. This paper describes the test vehicle flight, initial post flight trajectory, vehicle attitude estimation, and some initial test results.

2 Flight configuration and integration

The overall payload dimensions and the different payload modules are shown in Figure 3 and Figure 4. The experiments are carried out on the forward sections of payload including a cone, a cylinder, and a flare. The cone half angle of seven degrees was chosen to match configurations used in preceding ground tests and analytical/numerical work (Fig. 5). The flare angle of 33° was chosen to induce turbulent boundary layer separation and reattachment on the flare face. To measure key aerothermal parameters during flight these two parts, which represent the main scientific part of the payload, were instrumented with a large number of sensors. Behind the flare experiment service modules with a length of 800 mm was used containing the necessary electronic boxes for data acquisition.

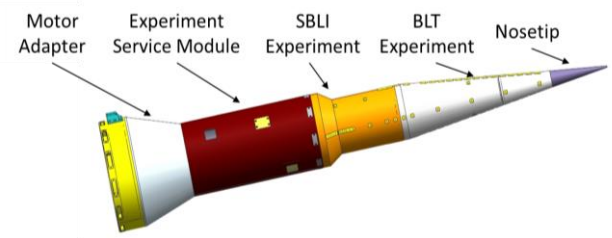

Figure 3. MF-1 payload overview.

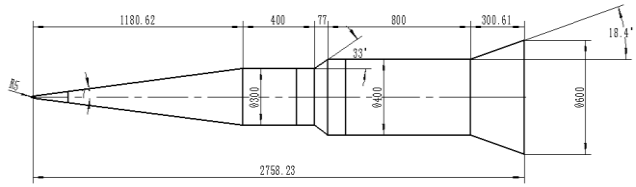

Figure 4. Payload geometry.

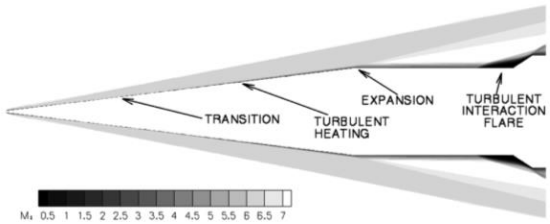

Figure 5. Overview of MF-1 payload flowfield.

The overall length of the payload including all service modules and motor adapter was 2758.23mm. This led to a total payload mass (including motor adapter and balance masses) of about 220 kg. The complete flight configuration with a length of 6.3 meter is shown in Fig. 6. The MF-1 vehicle was launched on an unguided rocket motor driven by solid propellant.

Figure 6. MF-1 complete configuration on assembly platform.

The main objective of the flight is to obtain the desired BLT and SBLI experimental data. For this to be achievable the payload must maintain its structural integrity until the end of the experiment. The payload had to be designed to withstand high aerodynamic heating loads resulting from hypersonic flight into a relatively dense atmosphere. The selected, parabolic, trajectory effectively limits the duration of in-atmosphere flight and consequent aero-thermal payload heating. As such it was possible to design the payload without having to add active or passive cooling systems and instead size the aero-shell walls to act as heat sinks. The nosetip stagnation region on the other hand reached temperatures approaching 1700K near the end of the trajectory. A high temperature alloy was used for the nosetip. The main body of the cone was made from stainless steel with a 12mm wall thickness. This thickness was chosen to provide sufficient heat sink mass for the duration of flight and still enable sufficient thermal response measurable with the chosen instrumentation. Located aft of the cone is a cylindrical section, required for isolation of the BLT and SBLI experiments. The cylinder section attaches to the cone section with blind fasteners, installed from the aft end of the cylinder. The cylinder was made from stainless steel and has a nominal wall thickness of 4.5mm. The flare section houses the SBLI experiment. The flare body was made from steel with 12mm to sustain higher temperatures on the flare face. The flare section attaches to the cylinder section using blind internal fasteners, similarly to the cone-cylinder joint. The payload on assembly platform is shown Fig. 7.

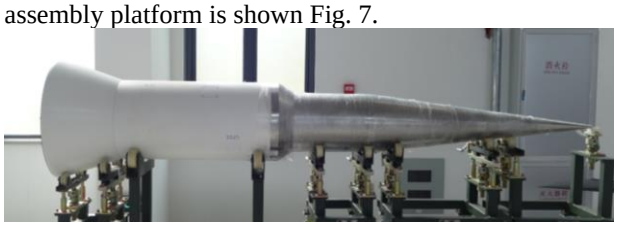

Figure 7. MF-1 payload on assembly platform.

The flight theory trajectory range was 224km, and the maximum altitude was 79.8km. The maximum flight Mach number was 5.53.

3 Instrumentation and data acquisition

3.1. Instrumentation

According to the theoretical prediction results of MF-1 boundary layer transition and shock boundary layer

interference, the temperature and pressure measurements on the surface of the payload were designed. The MF-1 flight experiment were equipped with overall 118 sensors, including 58 for temperature measurements， 60 for pressure measurements. The location of the instrumentation in cylindrical coordinates on the cone surface of the flight vehicle is shown in Figure 8. In this plot, Φ =0° is a body-referenced azimuthal coordinate, with Φ =0° coincident with the primary ray of thermocouple instrumentation. X axis is defined as the direction of the payload from the cone to the flare along the axis. The 58 temperature sensors were arranged at Φ =0°, 60°, 120° and 180°. The 60 pressure sensors were mainly concentrated near the cylinder-flare interface, to measure shock boundary layer interference. At x=800mm, 1400mm and 1580mm, 6 pressure sensors were arranged in the circumferential direction, the rest of sensors were equipped at Φ = 90° and 270°, and the starting point of the pressure measuring points was located at x=400mm.

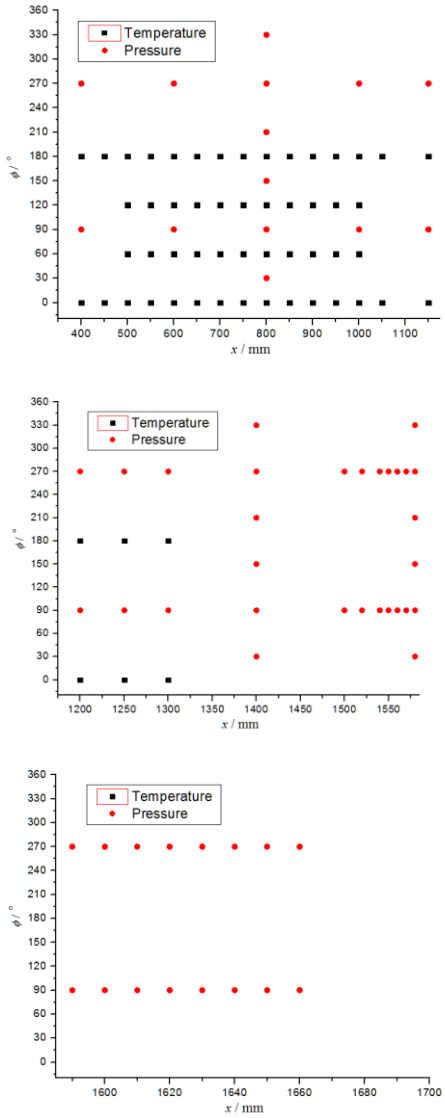

Figure 8. The location in cylindrical coordinates of the instrumentation on cone(up), cylinder(middle) and flare(down).

The optimization scheme of thin-skin model was used for temperature measurement structure. A thin-wall structure was designed for transition[14-15]. The measurement structure was shown in figure 9. The thermocouples were installed on backface of thin-wall. The outer surface temperature and heat flow data were obtained by data analysis and ground calibration. The thin-wall structure was welded with the payload structure. The solder joint has been polished to maintain aerodynamic shape after the welding was completed.

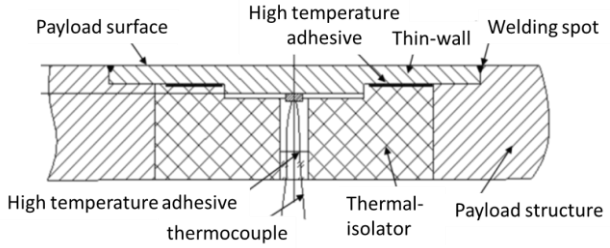

Figure 9. Thin-wall structure for temperature measurement.

The surface pressure measurement of payload used a pressure measurement system based on the electronic pressure scanner to measure 60 pressure data. A thin-wall structure was welded with payload at the measuring point. The solder joint has been polished after the welding was completed to maintain aerodynamic shape similarly to temperature measurement structure. Surface pressure was directed to the pressure scanner with stainless-steel tube and Polyvinylchlorid (PVC) tube. The structure of the pressure measurement is shown in Fig. 10

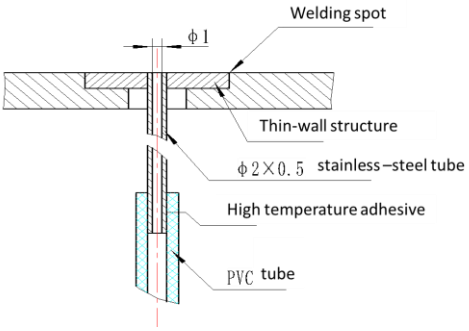

Figure 10. The surface pressure measurement structure.

3.2. Data acquisition

Data acquisition is carried out by means of telemetry emission recovery and data storage device recovery. The measurement data telemetry system collected sensor information such as temperature, pressure, Global Positioning System (GPS) and Inertial Measurement Unit （IMU）signal, and was received by ground equipment during the flight. Data storage device stored the measuring data during the flight and recovered the data after the flight test. The layout diagram of the telemetry equipment is shown Fig.11.

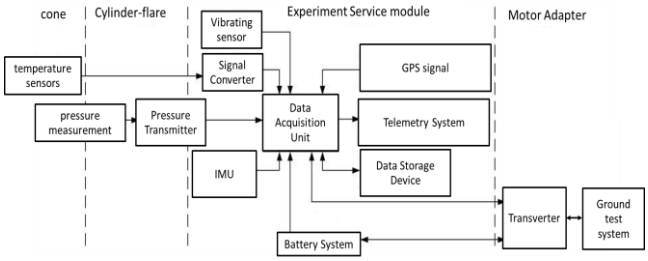

Figure 11. Data acquisition system of MF-1.

4. Flight data

4.1. Post flight trajectory

The MF-1 vehicle at the launcher is shown in Fig.12. The rocket stage accelerated the entire system with a total weight of 1739 kg to an altitude of 13.9 km as shown in Fig. 13. In the ascent phase the vehicle reached a maximum velocity of Ma 5.32 when the engine was shut off. The flight flew for 244.9 seconds. Data storage device was found after the flight. The debris of MF-1 is shown Figure 14.

Figure 12. MF-1 complete configuration at the launcher.

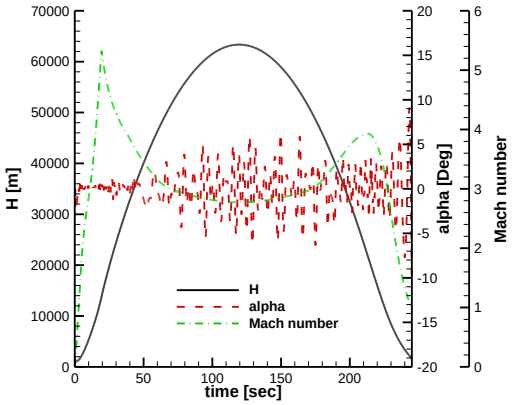

Figure 13. Flight trajectory of the MF-1 flight vehicle.

Figure 14. The debris of the MF-1 vehicle.

Fig. 15 shows a detailed view of Mach number (Ma) and Reynolds number (Re) during the experiment window within 10 to 30 seconds (ascent) and 210-230 seconds (descent). In the ascent, the flight Reynolds number decreases sharply due to the decrease in density as the altitude increases. However, due to the decrease of altitude and increase of density in the descending section, the flight Reynolds number gradually increases.

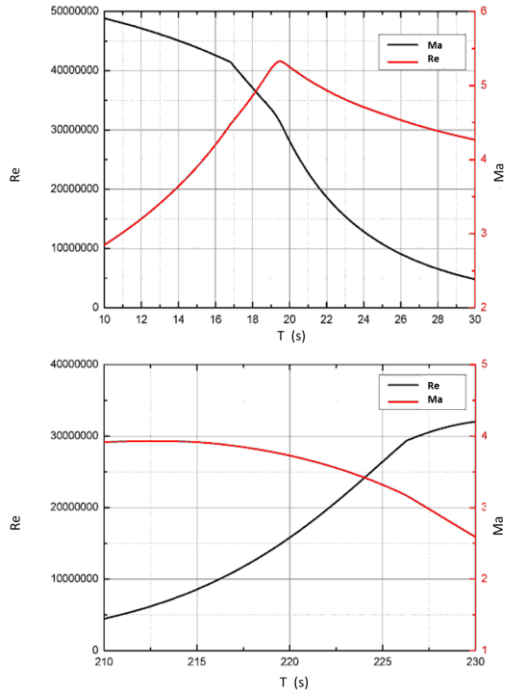

Figure 15. Flight Reynolds and Mach numbers during ascent(up) and decent(down).

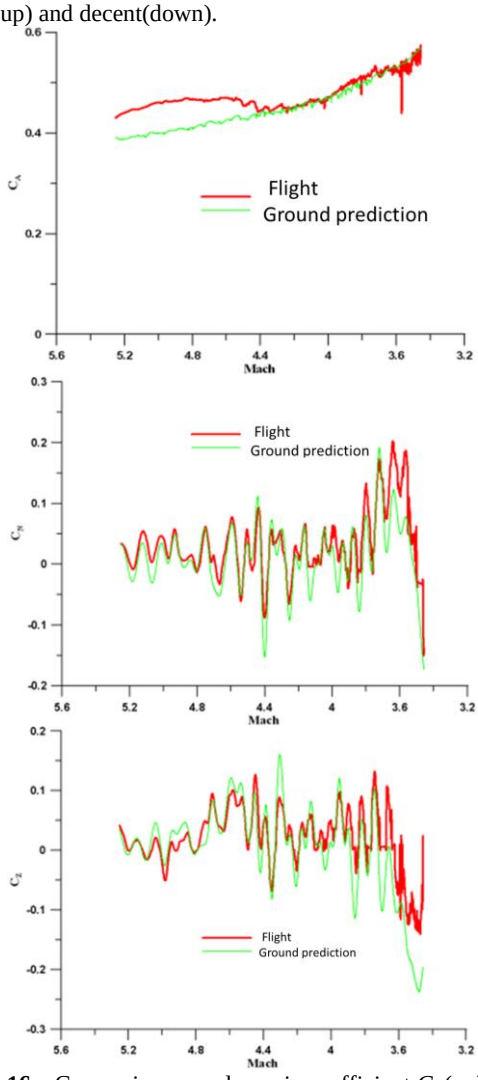

Figure 16. Comparison aerodynamic coefficient C_A(up), C_N(middle),and C_Z(down) between flight estimated and ground prediction.

The MF-1 flight data from data storage device was used to build an aerodynamic coefficient estimated. Compared this with the ground prediction data, and the results are shown in Fig. 16. When the Mach number was higher than 4.4, there would be a deviation in the axial aerodynamic coefficient (C_A) between flight results and the prediction of the ground, and the axial aerodynamic coefficient was higher in flight. The maximum deviation was more than 10%, but the trend was consistent. When the Mach number was less than 4.4 (22 km altitude above), The results of ground prediction were comparatively in agreement with flight. The normal aerodynamic coefficient (C_N) and lateral aerodynamic coefficient (C_Z) were consistent with the ground prediction results.

4.2. Heat Flux and Transition Result

The cone centerlines heat flux histories during the ascent and descent are shown in figures 17 and 18. As expected, the heat flux decreases as x increases and the boundary layer thickens. Jumps in heating rate due to transition are apparent at t = 16–22 and 215–223 s. The transition time remain basically unchanged along the cone surface at Φ =0° between x =450 mm and x =1150 mm. But，there are significant changes in transition time along the cone surface at Φ = 60°,120°,180°. At Φ =0°centerline, an unchanged transition time can be explained by roughness-induced transition causing turbulence on the leading edge to advance forward rapidly when the critical Reynolds number is reached.

To reveal greater detail than in the heating histories, the heating rates along the centerlines located Φ =0°,60°,120°,180 ° during the ascent and descent are shown in figures 19 and 20. The transition position changes significantly at different times along the cone surface at Φ =60°,120°,180 °. An unaltered point of transition is also considered to be a forced transition. The reason may be due to the assembly step between nosetip and cone.

4.3. Measured Surface Pressure Result

Although measuring transition (via temperature) was the primary objective of MF-1, the vehicle was instrumented with numerous pressure sensors to measure shock interaction as well. The measured pressure of flare surface at Φ =90 ° during ascend is shown in Fig. 21. However, the measured data may be inconsistent with the actual situation due to the improper measurement method. The measurement compared with Hifire-1 is shown in Fig. 26. The pressure oscillation phenomenon caused by shock boundary layer interaction did not appear in MF-1. The reason may be thought to be that the pressure measure tube was too long. The further details will be analysed and published.

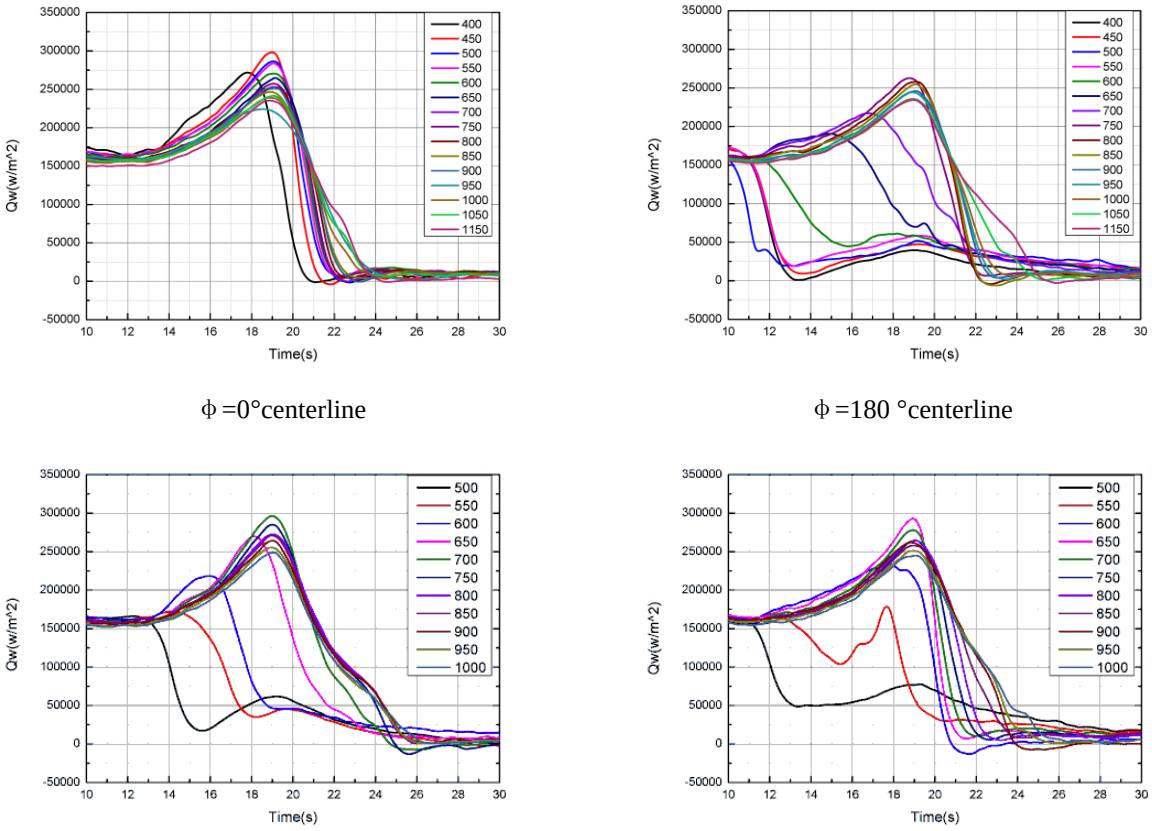

Figure 17. Φ =0°,60° ,120° and 180° centerlines heat flux during ascent(t=10-30s).

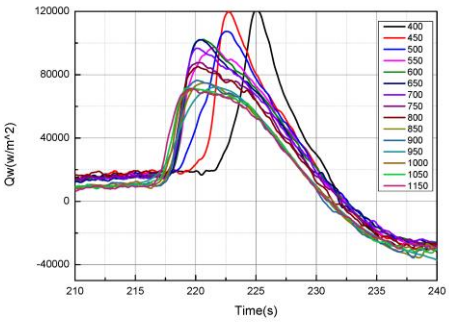

ϕ =0 ° centerline

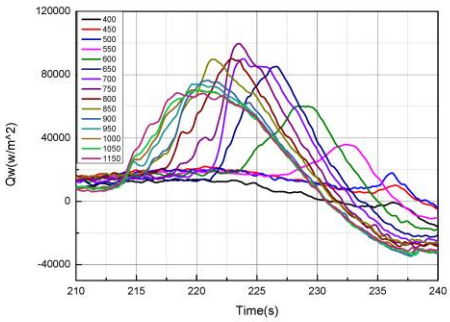

ϕ =180 °centerline

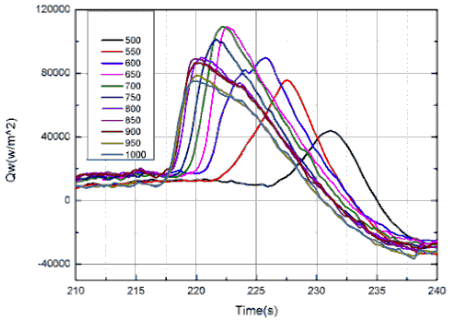

ϕ =60° centerline

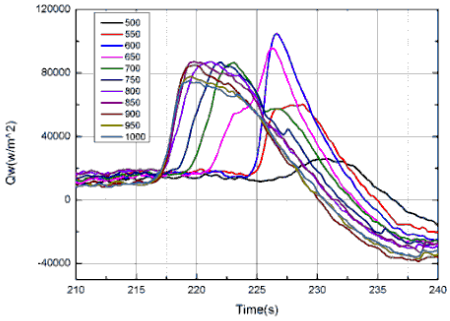

ϕ =120° centerline

Figure 18. ϕ =0°,60° ,120° and 180° centerlines heat flux during decent(t=210-230s).

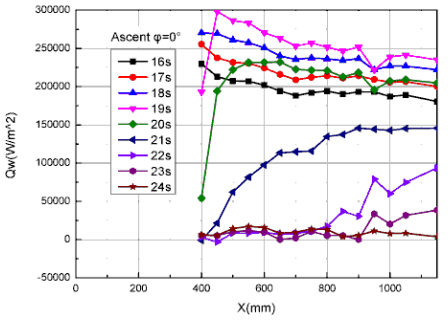

ϕ =0 ° centerline

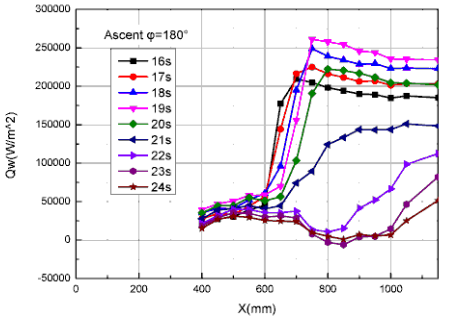

ϕ =180 ° centerline

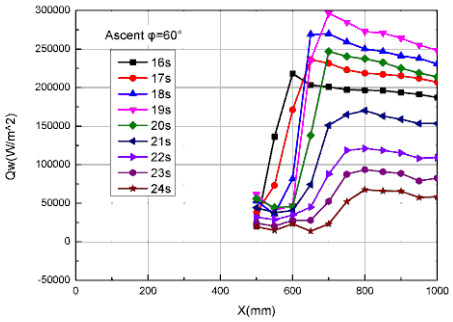

ϕ =60° centerline

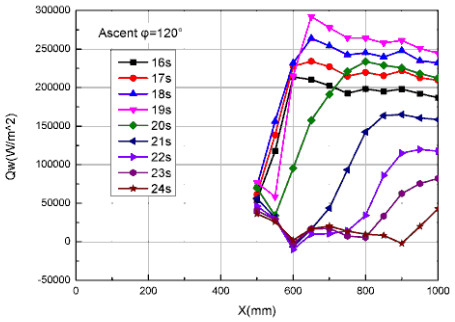

ϕ =120° centerline

Figure 19. ϕ =0°,60° ,120° and 180° centerlines transition during ascent(t=16-24s).

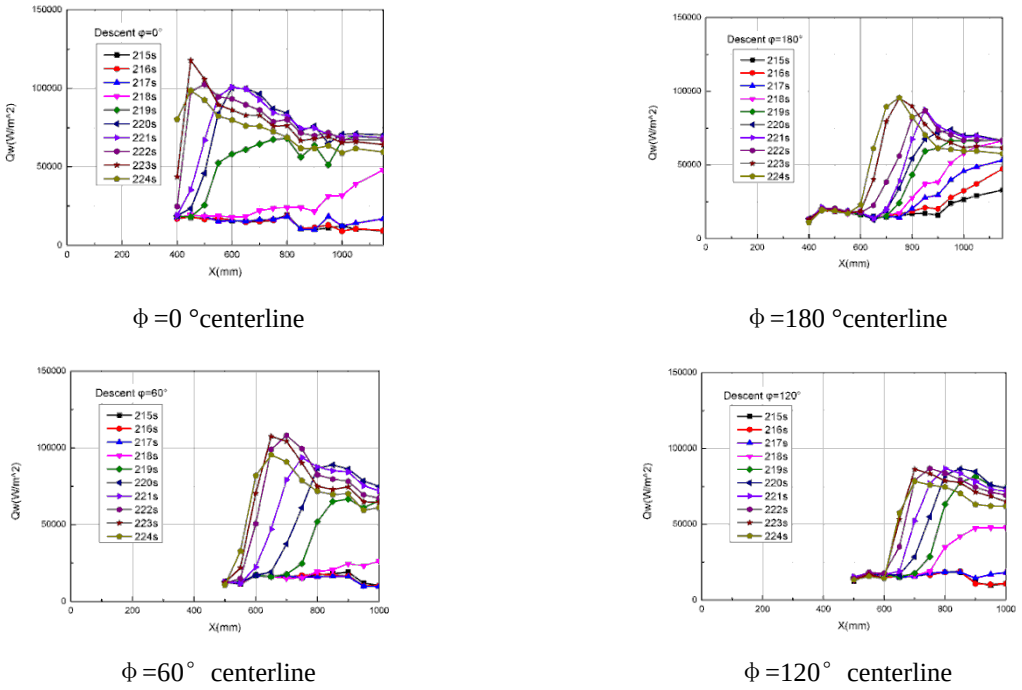

Φ =0 °centerline Φ =180 °centerline

Φ =60° centerline Φ =120° centerline

Figure 20. Φ =0°,60° ,120° and 180° centerlines transition during decent(t=215-223s).

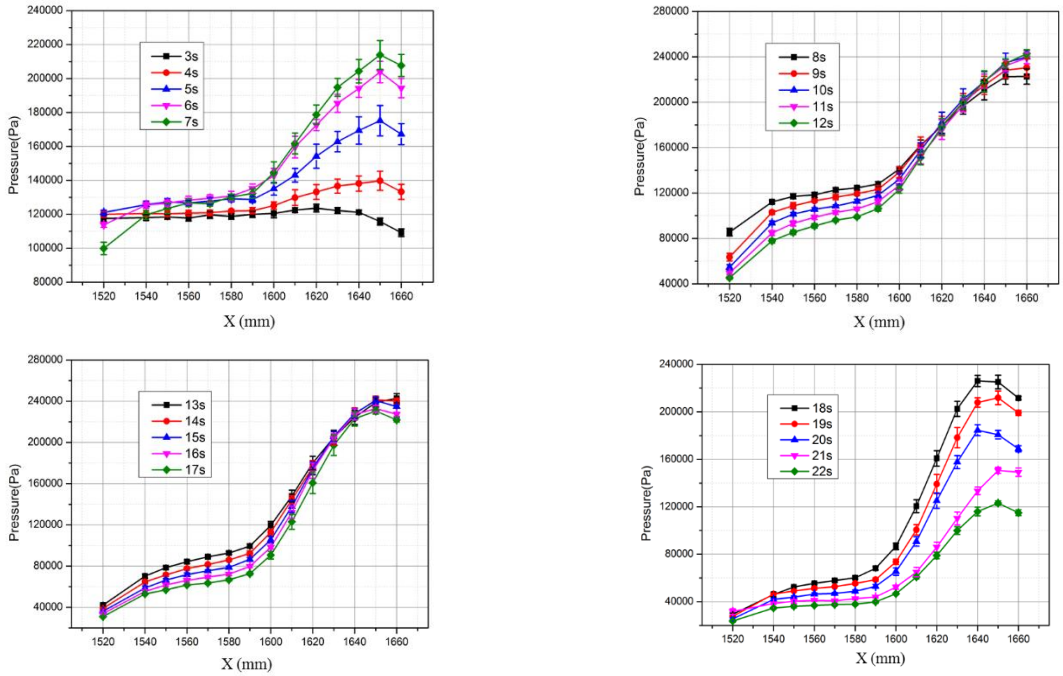

Figure 21. Φ =90°centerline flare surface pressure during ascent.

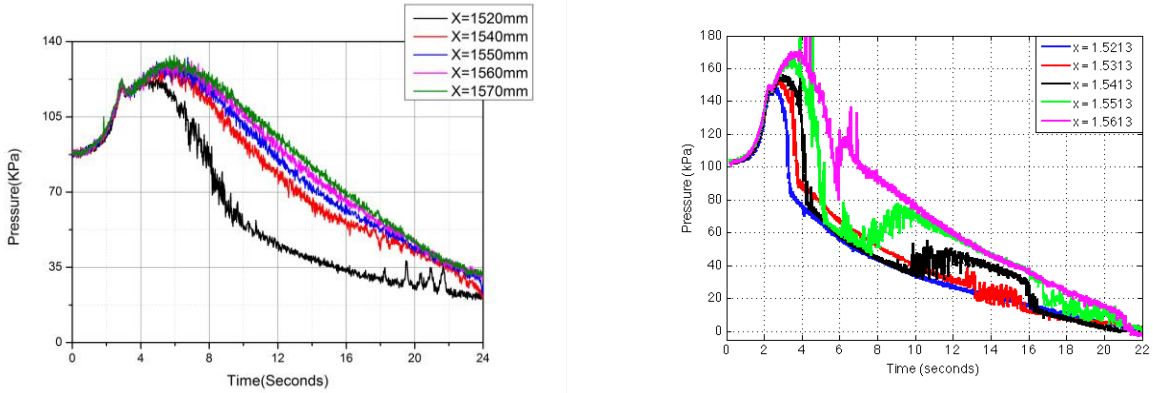

Figure 22 Compression flare surface pressure between MF-1(left) and Hifire-1(right) during ascent.

5 Conclusion

MF-1 was a highly successful flight for a “low-cost” flight experiment, 3+Gigabytes of data were obtained on boundary layer transition, shock boundary layer interactions as well as vehicle state data. Although MF-1was carried out as a low cost flight experiment without Control System and parachute system, the following important achievements were made:

-The launch, boost, tail and payload were carried out without any anomaly.

-The data acquisition systems worked perfect. The data storage device also worked well and all flight data were recovered. Most of the MF-1 instrumentation provided very useful data. The data can be used to verify the ground prediction method and calibration calculation model.

References

1. Ou C., JI H. L, Xiao H.S., et al. Key problems in structure and thermal protection for MF-1 model testing flight vehicle [J]. Acta Aerodynamica sinica, 2017,**35**(5):742-749.
2. Yang Q T, Zhou Y, Yuan X X, et al. Surface pressure and temperature measurement technology in MF-1 modelling flight test [J]. Acta Aerodynamica sinica, 2017,**35**(5):732-741.
3. He Z C, CHE J, XIAO H S, et al. Trajectory design and Monte Carlo flight simulation for MF-1 [J]. Acta Aerodynamica sinica, 2019,**37**(2):201-206.
4. Shehret Tilvaldyev, Erwin Martinez, Jorge Flores-Garay, and Alfredo Villanueva Montellano, "Distribution of Dynamic Pressure in Micro-Scale of Subsonic Airflow around Symmetric Objects at Zero Angle of Attack," International Journal of Mechanical Engineering and Robotics Research, Vol. **6**, No. 3, pp. 226-231, May 2017. DOI: 10.18178/ijmerr.6.3.226-231.
5. Yury I. Dimitrienko, Mikhail N. Koryakov, and Andrey A. Zakharov, "Computational Simulation of Conjugated Problem of External Aerodynamics and Internal Heat and Mass Transfer in High-Speed Aircraft Composite Construct," International Journal of Mechanical Engineering and Robotics Research, Vol. **6**, No. 1, pp. 58-64, January 2017. DOI: 10.18178/ijmerr.6.1.58-64
6. Kimmel, R. L. Aerothermal Design for the HIFiRE-1 flight Vehicle[C]. AIAA 2008-4034, June 2008.
7. Adamczak, D., Alesi, H., Frost, M. HIFiRE-1: Payload Design, Manufacture, Ground Test, and Lessons Learned[C]. AIAA paper 2009-7294, October 2009.
8. Roger L. Kimmel, David Adamczak. Hifire-1 Background and Lessons Learned[C]. AIAA paper 2012-1088, January 2012.
9. Schneider, S. P. Flight Data for Boundary-Layer Transition at Hypersonic and Supersonic Speeds[J]. Journal of Spacecraft and Rockets, vol. **36**, no. 1, January-February 1999.
10. Stetson, K. F. Nosetip Bluntntess Effects on Cone Frustum Boundary Layer Transition in Hypersonic Flow[C]. AIAA paper 83-1763, July 1983.
11. Kimmel, R. L., Adamczak, D., Gaitonde, D., Rougeux, A., Hayes, J. R., HIFiRE-1 Boundary Layer Transition Experiment Design[C]. AIAA paper 2007-0534, January 2007.
12. Johnson, H. B., Alba, C. R., Candler, G. V., MacLean, M., Wadhams, T, and Holden, M. Boundary Layer Stability Analysis of the Hypersonic International Flight Research Transition Experiments[C]. AIAA Journal of Spacecraft and Rockets, vol. **45**, no. 2, March-April 2008.
13. Stainback, C. P. Effect of Unit Reynolds Number, NoseBluntness, Angle of Attack, and Roughness on Transition on a 5°Half-Angle Cone at Mach 8[C]. NASA TN D-4961, January 1969.
14. LIU CHU-ping,YANG Qing-tao， et al. Heatflux measurement in aerothermodynamics and thermal protection tests [M]. Beijing:National Defense Industry Press,2013.
15. ZHANG Shou-yan,HUI Yu-xin， et al. Modeling Free flight [M]. Beijing: National Defense Industry Press,2002.